RESEARCH ARTICLE
doi: 10.2306/scienceasia1513-1874.2025.094

ScienceAsia 51 (6): 2025: ID 2025094: **1–10**

In vitro and *in silico* evaluation of α-glucosidase and α-amylase inhibitory effects of *Etlingera elatior* flower extracts and HPLC method validation for marker analysis

Weerachai Pipatrattanaseree[a,*], Supaluck Nuaeissara[b], Sakwichai Ontong[c], Aussavashai Shuayprom[a], Thana Juckmeta[d,*]

[a] Regional Medical Sciences Center 12 Songkhla, Department of Medical Sciences, Ministry of Public Health, Songkhla 90100 Thailand

[b] Center of Excellence on Applied Thai Traditional Medicine Research, Faculty of Medicine, Thammasat University, Pathum Thani 12120 Thailand

[c] Medical Plant Research Institute, Department of Medical Sciences, Ministry of Public Health, Nonthaburi 11000 Thailand

[d] Chulabhorn International College of Medicine, Thammasat University, Pathum Thani 12120 Thailand

[*]Corresponding authors, e-mail: weerachai.tu2557@gmail.com, thanajuckmeta9@gmail.com

Received 2 Dec 2024, Accepted 31 Oct 2025
Available online 22 Dec 2025

ABSTRACT: The flowers of *Etlingera elatior*, an edible plant belonging to the Zingiberaceae family, have been traditionally recognized in folk medicine for their potential to reduce the risk of diabetes. In this study, we investigated *in vitro* and *in silico* α-glucosidase and α-amylase inhibitory activities of various extracts from *E. elatior* flowers and their major markers. Additionally, we validated an HPLC analysis. Fresh and dried *E. elatior* flowers were extracted by decoction and maceration. The extracts and the two markers, chlorogenic acid and rutin, were evaluated through α-glucosidase and α-amylase inhibitory assays. Molecular docking study was used to predict binding affinity and ligand-protein interactions. A quantitative HPLC method was validated following the ICH guidelines. The 70% ethanolic extract from fresh *E. elatior* flowers exhibited the highest α-glucosidase inhibitory activity (IC_{50} = 203.35 ± 27.91 µg/ml), while none of the extracts showed significant effects on α-amylase. Both chlorogenic acid and rutin showed potential against α-glucosidase, but not against amylase. Rutin inhibited α-glucosidase with a lower IC_{50} value than acarbose (85.59 ± 4.50 vs. 121.14 ± 7.22 µg/ml). *In silico*, rutin demonstrated a higher binding affinity to α-glucosidase than acarbose (−10.4 and −9.0 kcal/mol, respectively). Enzyme-ligand interactions revealed that all compounds bound to catalytic residues at the enzyme's active site. The HPLC method for determining chlorogenic and rutin showed good validation results. This study revealed the presence of α-glucosidase inhibitory markers in *E. elatior* flowers, and the validated HPLC method can be utilized for the quality control of *E. elatior* flower extracts.

KEYWORDS: *Etlingera elatior*, α-glucosidase, rutin, chlorogenic acid, method validation

INTRODUCTION

Diabetes mellitus (DM) is a chronic metabolic disease contributing to uncontrollable blood sugar. It is classified into type I, type II, and gestational diabetes mellitus. Type II diabetes is the most common form [1]. Managing diabetes involves controlling blood glucose levels and preventing complications. One approach is the inhibition of carbohydrate absorption in the gastrointestinal tract by targeting carbohydrate-digesting enzymes, such as α-glucosidase and α-amylase, which break down carbohydrates into absorbable sugars [2]. Synthetic inhibitors like acarbose, miglitol, and voglibose are effective but often cause side effects such as nausea and diarrhea [3, 4]. Therefore, natural sources for these enzyme inhibitors with fewer side effects are continuously explored.

Etlingera elatior (Jack) Smith, commonly known as torch ginger, is a plant belonging to the Zingiberaceae family. It is widely cultivated in Southeast Asia and other tropical regions [5]. In Thailand and Malaysia, the flowers of torch gingers are consumed both raw and cooked and are also processed into juice [6]. Malaysian folk medicine takes the raw flowers to reduce the risk of diabetes and hypertension [7]. Several pharmacological activities of *E. elatior* have been reported including antioxidant, antibacterial, cytotoxic [6], anti-inflammation [7], and anti-aging properties [8]. Screening of phytochemicals of *E. elatior* flowers revealed the presence of flavonoids, terpenoids, saponins, tannins, and anthocyanins [9]. An aqueous extract of *E. elatior* flowers exhibited a high percentage of α-glucosidase and α-amylase inhibition, suggesting that its phenolic and flavonoid contents contributed to the enzyme inhibition [10]. Other *in vitro* studies reported that rutin showed an anti-α-glucosidase effect [11]; moreover, phenolic and flavonoid compounds such as chlorogenic acid and rutin exhibited anti-diabetic activity in type II diabetic rat models [12]. Nevertheless, the marker compounds of *E. elatior* flowers responsible for α-glucosidase and α-amylase inhibition have not yet been identified.

Phytochemical analysis of secondary metabolites of *E. elatior* flowers, including gallic acid, tannic acid,

chlorogenic acid, quercetin, apigenin, kaempferol, luteolin, and myricetin, was performed using the UHPLC method [6]. Another study reported an HPLC analysis of chlorogenic acid in the leaves of *E. elatior* but did not include validation results [13]. A recent study presented a method for extracting, separating, isolating, and identifying components in the leaves of *E. elatior* using pressurized matrix solid-phase dispersion in combination with liquid chromatography-mass spectrometry (LC-MS) [14]. A partially validated HPLC method by Firdhauzi et al determined only chlorogenic acid with antioxidant activity [15]. Our previous research on the anti-aging and wound-healing properties of *E. elatior* extracts identified chlorogenic acid and rutin as markers, although the HPLC method lacked validation [16]. Recently, there are no reports indicating the α-glucosidase and α-amylase inhibitory markers of the *E. elatior* flowers, nor is there any report on method validation for the quality control of *E. elatior* flower extracts.

The purpose of the present study was to evaluate *in vitro* α-glucosidase and α-amylase inhibitory activities of various *E. elatior* flower extracts, as well as in the markers, chlorogenic acid and rutin. Additionally, the interactions between these compounds and the enzymes were studied *in silico*. Finally, the HPLC method was validated for quality control purposes.

MATERIALS AND METHODS

Plant materials and preparations

E. elatior was collected from Yala Province, Thailand, in December 2020 and authenticated by Mr. Sakwichai Ontong, the Medical Plant Research Institute, Department of Medical Science, Thailand. The plant specimen (voucher number DMSC 5256) was deposited at the Department of Medical Sciences Herbarium (DMSC), the Department of Medical Sciences, Nonthaburi, Thailand.

The collected inflorescences of *E. elatior* were washed, and the edible parts—including the floral bract, involucral bract, and true flower—were removed from the receptacle and combined. This mixture, referred to as the crude flower, was then dried in a hot air oven at a temperature of 45 °C. Both the fresh and dried crude flowers were separately extracted using two methods: maceration and decoction. For maceration, the crude flowers were macerated in 95% ethanol, 70% ethanol, and 50% ethanol (3 days × 3 times). Each extract was filtered and evaporated under reduced pressure at a temperature below 45 °C. For decoction, the crude flowers were boiled in distilled water for 15 min and then filtered with filter paper. The residue was re-extracted twice using the same process. The aqueous solutions were combined and dried using a freeze dryer to obtain water extracts. All samples were stored at −20 °C until use.

Chemicals and reagents

Chlorogenic acid (purity 97.2%) and rutin (purity 95.0%) were purchased from Sigma (Darmstadt, Germany). Trifluoroacetic acid, ethanol, and methanol (HPLC grade) were purchased from Labscan (Bangkok, Thailand). Purified water was prepared by the Milli Q® system from Millipore (Bedford, MA, USA). α-glucosidase, α-amylase, *p*-nitrophenyl α-D-glucopyranoside (*p*-NPG), starch, potassium sodium tartrate, tetrahydrate, and 3,5-Dinitrosalicylic acid were purchased from Sigma.

In vitro inhibitory effect on α-glucosidase

The *in vitro* α-glucosidase inhibitory activity of *E. elatior* extract was assessed following a modified method by Gowri et al [17]. Hydro-alcoholic extracts were dissolved in DMSO, and aqueous extracts in water, both at a stock concentration of 10 mg/ml. Working solutions were prepared at concentrations of 100–10,000 µg/ml using phosphate buffer. DMSO (10% in buffer) was utilized as the control for the hydro-alcohol extract, and water was used for the aqueous extract. The enzymatic reaction was carried out by mixing 80 µl of phosphate buffer (pH 6.8), 20 µl of sample solution, and 50 µl of α-glucosidase (0.15 U/ml) in a 96-well plate, followed by incubation at 37 °C for 15 min. Next, 50 µl of the substrate (5 mM *p*-nitrophenyl α-D-glucopyranoside) was added, mixed, and incubated for another 15 min. The enzyme reaction was terminated by adding 100 µl of 1 M Na_2CO_3. The product (*p*-nitrophenol) was measured at 405 nm using a microplate reader. The inhibitory activity was calculated, and IC_{50} values were determined through curve fitting regression analysis using GraphPad Prism 5.0 (CA, USA).

$$\text{Inhibition}(\%) = \frac{(\text{OD}_{\text{control}} - \text{OD}_{\text{sample}})}{\text{OD}_{\text{control}}} \times 100$$

where $\text{OD}_{\text{control}}$ represents the optical density of control sample, and $\text{OD}_{\text{sample}}$ represents the optical density of the tested sample.

In vitro inhibitory effects on α-amylase

The α-amylase inhibitory activity of *E. elatior* extract was evaluated using a modified method by Ademiluyi et al [18]. Hydro-alcoholic extracts were dissolved in DMSO, and aqueous extracts were dissolved in water, both at a stock concentration of 10 mg/ml. Working solution was prepared at 5,000 µg/ml by diluting the stock solution with phosphate buffer. In a reaction microtube, 50 µl of the sample solution was mixed with 50 µl of α-amylase (0.5 mg/ml in phosphate buffer, pH 6.9) and 100 µl of 0.02 M sodium phosphate buffer (pH 6.9) containing 0.006 M sodium chloride. The mixture was incubated at 37 °C for 10 min. Then, 50 µl of 1% starch solution (in phosphate buffer, pH 6.9) was added and incubated for 20 min. The reaction was stopped by adding 100 µl of

DNS reagent (96 mM 3,5-dinitrosalicylic acid, 3.5 M sodium potassium tartrate in 2 M NaOH). The mixture was heated at 90–100 °C for 5 min, cooled on ice for 5 min, and diluted with 650 µl of water. A 200-µl aliquot of the reaction mixture was transferred to a 96-well plate, and the absorbance was measured at 540 nm using a microplate reader. The percentage inhibition was calculated, and IC_{50} values were determined using curve-fitting regression analysis with GraphPad Prism.

$$\text{Inhibition}(\%) = \frac{(\text{OD}_{\text{control}} - \text{OD}_{\text{sample}})}{\text{OD}_{\text{control}}} \times 100$$

where $\text{OD}_{\text{control}}$ represents the optical density of control sample, and $\text{OD}_{\text{sample}}$ represents the optical density of the tested sample.

Molecular docking study

The crystallographic structures of the enzymes used in the molecular docking study were obtained from the Brookhaven Protein Data Bank (RCSB PDB, http://www.rcsb.org) [19]. Porcine pancreatic α-amylase (PDB ID: 1OSE) [20] and human pancreatic α-amylase (PDB ID: 3BAJ) [21] were selected for molecular docking for α-amylase enzyme. *Saccharomyces cerevisiae* α-glucosidase (PDB ID: 3A4A) [22] and human α-glucosidase (PDB ID: 3L4Y) [23] were used for α-glucosidase.

The 3D structures of acarbose, chlorogenic acid, and rutin were retrieved from the PubChem (Compound ID: 41774, 1794427, and 5280805) [24]. Ligand was prepared by PyRx-Python 0.8 [25], with energy minimization and conversion to AutoDock file format (pdbqt) via Open Babel. Protein preparation was performed using Discovery Studio 2021 by removing water molecules and bound ligands, adding polar hydrogens, and converting to pdbqt in PyRx-Python 0.8. The docking grid center was based on the coordinates of the co-crystallized ligand (Table S1). Docking was performed in PyRx with AutoDock Vina (exhaustiveness set to 50), and results were visualized in Discovery Studio 2021.

To verify the docking protocol, native ligands were re-docked with their corresponding proteins, and the root mean square deviation (RMSD) between the re-docked and the native ligand poses was calculated by comparing the atomic distances using Discovery Studio 2021. All the RMSD values of the re-docked ligands were less than 2.0 Å (Fig. S1).

Determination of chlorogenic acid and rutin by HPLC

The HPLC method for simultaneously determining chlorogenic acid and rutin in *E. elatior* extract was based on our previously unvalidated protocol [16]. This study validated the method following ICH guidelines [26], including specificity, linearity, range, limit of detection (LOD), limit of quantitation (LOQ), accuracy, and precision.

The determination of chlorogenic acid and rutin in *E. elatior* extract was carried out using a Dionex® Ultimate 3000 RS HPLC system (Dionex®, USA) The phytochemicals in extracts were separated on a BDS Hypersil® C18 column (4.6 mm × 150 mm, 5 µm) with a gradient elution of the mobile phase consisting of 0.1% v/v trifluoroacetic acid (solvent A) and methanol (solvent B). The gradient program was as follows: 0–5 min, 95%A: 5%B; 5–20 min, 95–75%A: 5–25%B; 20–30 min, 75–30%A: 25–70%B; 30–35 min, 30%A: 70%B; 35–40 min, 95%A: 5%B [16]. Five microliters of the prepared solutions were injected into the chromatographic system, and the detector was set at a wavelength of 257 nm. Stock solutions of chlorogenic acid and rutin (1 mg/ml) were prepared in methanol. Working solutions and sample solutions were prepared in methanol and filtered through a 0.45 µm membrane before HPLC injection.

Validation of the HPLC method

The specificity of the method was assessed by comparing chromatograms of blank (methanol), standard, and sample solutions, with the UV spectra of peaks in sample chromatograms matching those of the standard. The UV spectrum of each analyzed peak in the sample solution at peak-start, peak-apex, and peak-end presented a similar pattern. The linearity of each compound's calibration curve was determined by the coefficient of determination (r^2) across six concentration levels of chlorogenic acid and rutin. The LOD and LOQ of each compound were evaluated based on the visualization method by diluting the standard mixture solution. LOD and LOQ were calculated based on three and ten times the signal-to-noise ratio, respectively. Accuracy (% recovery) and precision (% CV) were evaluated using QC samples spiked at low, medium, and high concentrations, with triplicate analyses over three consecutive runs. The intermediate precision was investigated by analyzing the QC samples by different days (three days), two columns, and two HPLC instruments.

Statistical analysis

All experiments were conducted in triplicate, and the results were reported as mean ± standard deviation (SD). The IC_{50} values were calculated by using a regression analysis. The differences between groups were statistically analyzed using one-way ANOVA with Tukey's test for post hoc analysis. GraphPad Prism software (CA, USA) was utilized for statistical analysis.

RESULTS

The extraction yields (%) of fresh and dried *E. elatior* flowers are shown in Table 1. The 95% ethanol extract showed the highest yield in both fresh and dried crude

Table 1 Extraction methods and yields of *E. elatior* extracts.

Crude flower	Code	Extraction solvent	Extraction method	Extraction Yield (%)
Fresh	EF-W	Water	Decoction	1.5
	EF-50	50% Ethanol	Maceration	1.5
	EF-70	70% Ethanol	Maceration	2.0
	EF-95	95% Ethanol	Maceration	2.5
Dry	ED-W	Water	Decoction	15.8
	ED-50	50% Ethanol	Maceration	16.7
	ED-70	70% Ethanol	Maceration	18.9
	ED-95	95% Ethanol	Maceration	20.0

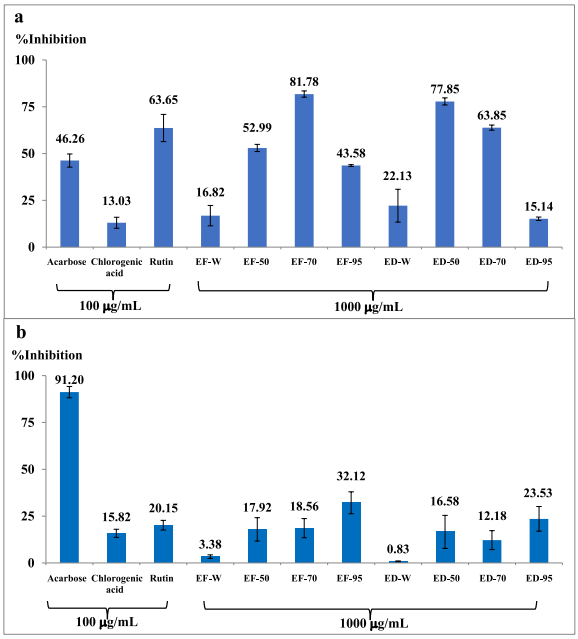

Fig. 1 Inhibitory activity of *E. elatior* extracts (1,000 µg/ml) and pure compounds (100 µg/ml) against α-glucosidase (a) and α-amylase (b).

flowers, whereas the decoction extracts showed the lowest extraction yields.

Effects of *E. elatior* extracts on α-glucosidase and α-amylase

The inhibitory effects of *E. elatior* extracts on α-glucosidase and α-amylase were evaluated at a concentration of 1,000 µg/ml prior to determining the IC_{50} values, and the extracts exhibiting greater than 50% inhibition were selected for IC_{50} investigation (Fig. 1). For α-glucosidase, the EF-70 exhibited the highest inhibitory activity (203.35 ± 27.91 µg/ml), followed by ED-50 and ED-70. Rutin showed stronger inhibitory activity compared to the positive control, acarbose (Table 2). Regarding α-amylase, all extracts exhibited less than 50% inhibitory activity at a concentration of 1,000 µg/ml (Fig. 1). Acarbose exhibited the highest inhibitory with 91.20 ± 3.02% inhibition at a concentration of 100 µg/ml. The IC_{50} values of acarbose, chlorogenic acid, and rutin were 7.43 ± 0.71 µg/ml (10.84 µM), 655.23 ± 17.85 µg/ml (1,849.36 µM), and 262.57 ± 8.96 µg/ml (430.08 µM), respectively (Table 2).

Molecular docking

The 3D models of α-glucosidase with the docked ligands at their active sites are displayed in Fig. 2 and Fig. S2 for α-amylase. The binding energies and interaction types from the molecular docking study are summarized in Table S2. The enzymes used in our *in vitro* experiments were compared with their human counterparts. Rutin exhibited the highest binding affinity to all enzymes, while chlorogenic acid and acarbose showed comparable binding affinities.

The binding interactions of the ligand-protein complexes revealed the types of chemical bonds between the ligands' functional groups and protein residues (Fig. 3 and Fig. S3). Acarbose and chlorogenic acid predominantly formed hydrogen bonds with amino acid residues, whereas rutin interacted through both hydrogen bonds and hydrophobic interactions. Unfavorable interactions were observed in the docking of all enzymes, except for 3L4Y. Compared to acarbose, rutin exhibited a higher number of molecular interactions and lower binding energy in all docked enzymes, while chlorogenic acid displayed fewer interactions and higher binding energy.

Method validation

In this study, we validated our previously developed HPLC method for the determination of chlorogenic acid and rutin in *E. elatior* extract [16]. Chlorogenic acid and rutin were identified as the two major compounds in the chromatogram, with retention times of 19.2 and 27.4 min, respectively (Fig. 4). The retention times and UV spectra of chlorogenic acid and rutin peaks in the sample solution corresponded to those in the standard solution (Fig. 4, Fig. S4a and Fig. S4b). No interference was observed in the chromatogram of the blank at the retention times of the analytes. The UV spectrum at peak-start, peak-apex, and peak-end of each peak showed a similar pattern (Fig. S4c and Fig. S4d), which supports the specificity and selectivity of the method. The linear concentration range was 20–250 µg/ml for chlorogenic acid and 5–100 µg/ml for rutin, with the coefficient of determination (r^2) exceeding 0.999. The LOD and LOQ for chlorogenic acid and rutin are presented in Table S3 and Fig. S5. Accuracy, expressed as % recovery, ranged from 97.0% to 105.2%, and the relative standard deviation (RSD, %) for precision was less than 2.0% (Table 3). The intermediate precision was investigated by analyzing the samples on different days, using different columns, and with different instruments. The %RSD for between-day precision of both compounds was below 2.0%. The relative percent differences (RPD, %) for chlorogenic

Table 2 Inhibitory activity of *E. elatior* extracts against α-glucosidase.

Extract/Compound		IC_{50} (μg/ml; mean ± SD)	
		α-glucosidase	α-amylase
Fresh crude flower extract	EF-W	>1000[a]	>1000[e]
	EF-50	740.57 ± 101.60[b]	>1000[e]
	EF-70	203.35 ± 27.91[c]	>1000[e]
	EF-95	>1000[a]	>1000[e]
Dried crude flower extract	ED-W	>1000[a]	>1000[e]
	ED-50	416.98 ± 51.92[d]	>1000[e]
	ED-70	419.94 ± 54.41[d]	>1000[e]
	ED-95	>1000[a]	>1000[e]
Pure compound	Chlorogenic acid	199.13 ± 4.50[c] [0.56 mM]	655.23 ± 17.85[f] [1.85 mM]
	Rutin	85.59 ± 7.31[c] [0.14 mM]	262.57 ± 8.96[g] [0.43 mM]
	Acarbose	121.14 ± 7.22[c] [0.19 mM]	7.43 ± 0.71[h] [0.011 mM]

Different alphabets above the IC_{50} values showed statistically significant difference (p-value<0.05), calculated by Tukey's multiple comparison test. (α-glucosidase: a–d; α-amylase: e–h)

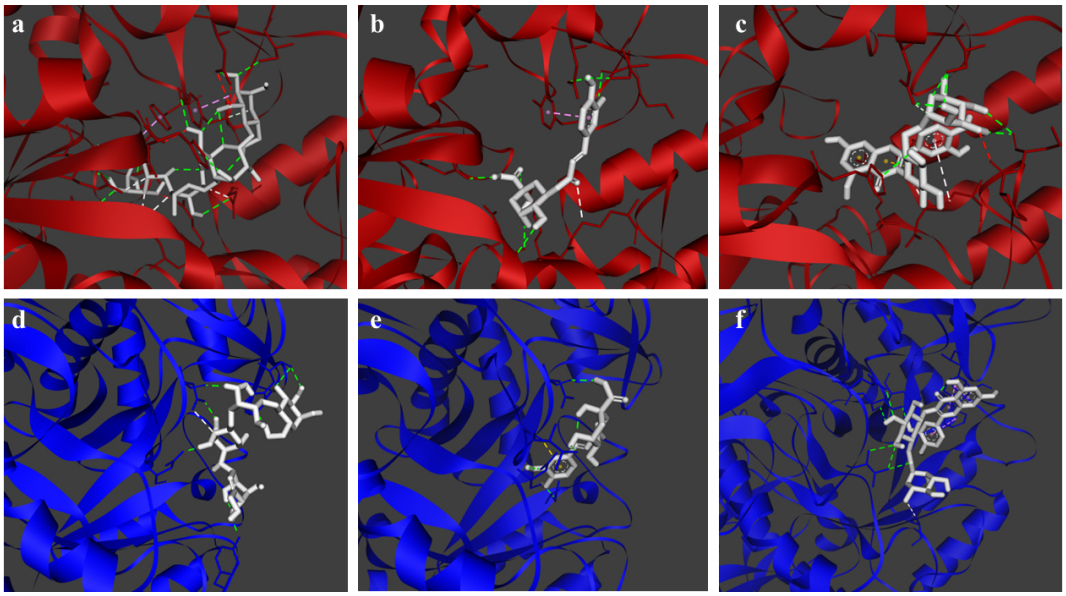

Fig. 2 3D models of α-glucosidase with docked ligands at the active sites. Proteins: (a–c) porcine *S. cerevisiae* α-glucosidase (3A4A) and (d–f) human pancreatic α-glucosidase (3L4Y). Ligands: acarbose (a, d); chlorogenic acid (b, e); rutin (c, f).

acid between columns and instruments were less than 3.51% and 3.36%, respectively. For rutin, the %RPD values were less than 5.62% and 3.76%, respectively (Table S4).

Determination of chlorogenic acid and rutin in *E. elatior* extracts

The chlorogenic acid and rutin contents in *E. elatior* extracts are showed in Table 4. The ED-50 contained the highest content of chlorogenic acid (9.46 ± 0.55 mg/g) while the EF-95 showed the lowest content (0.99 ± 0.07 mg/g). For rutin, the highest contents were found in ED-70 and ED-50 (3.10 ± 0.16 and 3.09 ± 0.11 mg/g, respectively), whereas the lowest concentration was in EF-W (0.96 ± 0.07 mg/g). Overall, the dried crude flower extracts exhibited higher levels of both chlorogenic acid and rutin compared to the fresh crude flower extracts when similar extraction methods were used.

DISCUSSION

The flower of *E. elatior* has been used as an edible vegetable and herbal medicine [11]. In this study, *E. elatior* extracts were investigated for α-glucosidase and α-amylase inhibition, with chlorogenic acid and rutin selected as markers due to their major peaks in the HPLC chromatogram.

EF-70 showed the highest α-glucosidase inhibitory activity, comparable to the positive control, acarbose. However, all the extracts exhibited low inhibitory activity against α-amylase. Differences with a previous

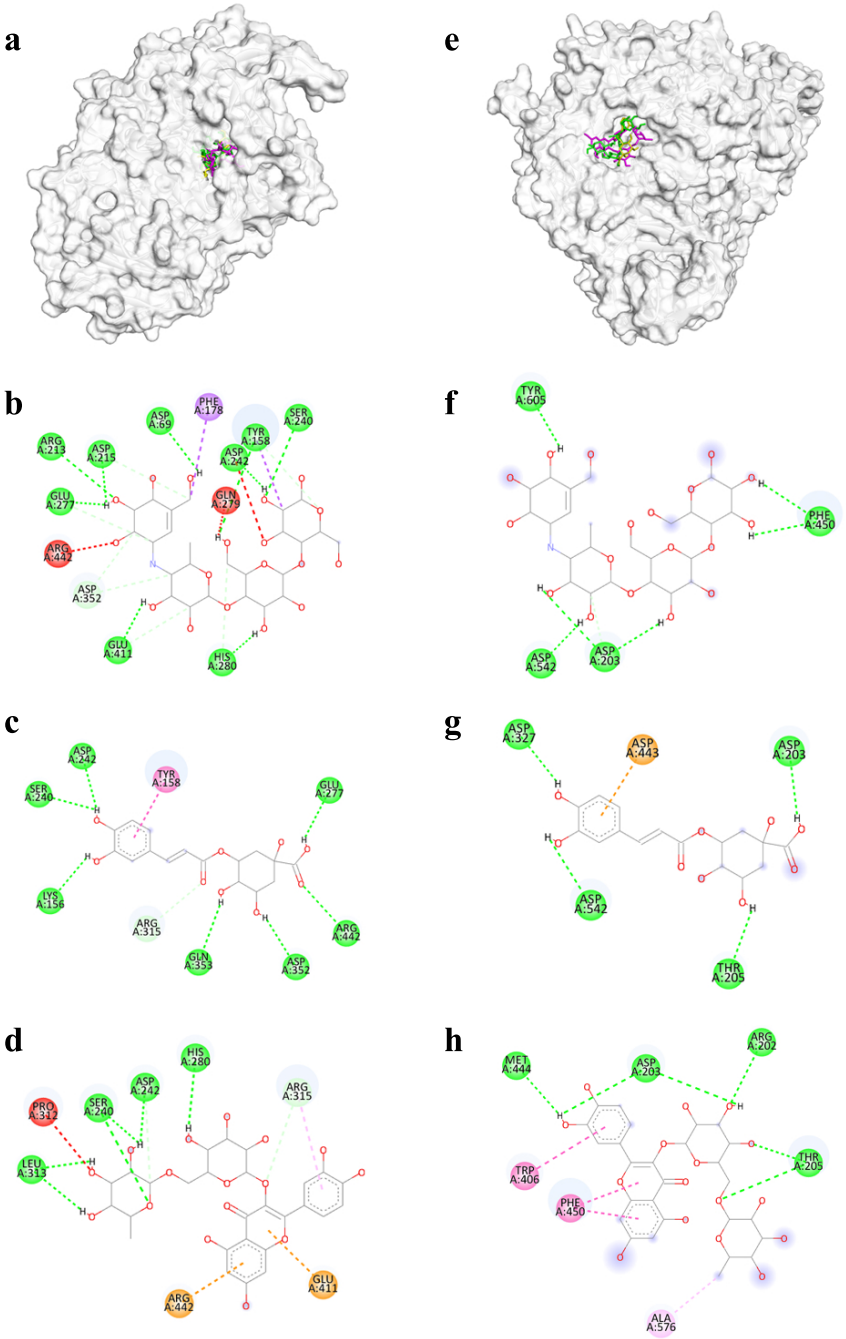

Fig. 3 3D models of α-glucosidase with docked ligands (acarbose, chlorogenic acid, and rutin) at the active sites: (a) *S. cerevisiae* α-glucosidase (3A4A) and (e) human pancreatic α- glucosidase (3L4Y). 2D predicted binding interactions of chlorogenic acid, rutin, and acarbose at the active sites of 3A4A (b, c, and d, respectively) and 3L4Y (f, g, and h, respectively). Types of ligand-protein interaction are indicated by color: green = hydrogen bonding; pink = Pi-Pi stacked; pale pink = Pi-alkyl; purple = Pi-Sigma; brown = Pi-Anion; red = unfavorable acceptor-acceptor or donor-donor.

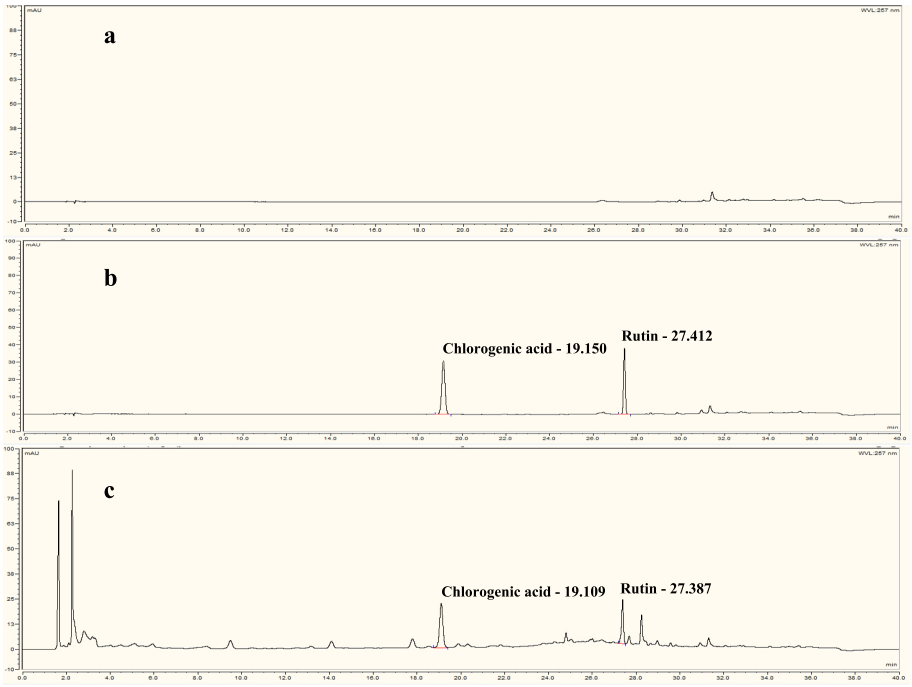

Fig. 4 HPLC chromatograms of blank (a), standard solution (b), and sample solution (c).

Table 3 Accuracy and precision of the method.

Compound	Spiked concentration (µg/ml)	Concentration found (µg/ml; Mean ± SD)	RSD (%)	% Recovery
Within-run ($n = 3$)				
Chlorogenic acid	40	39.61 ± 0.70	1.77	97.4% – 104.5%
	80	81.06 ± 1.32	1.64	
	150	156.59 ± 0.22	0.14	
Rutin	10	9.91 ± 0.06	0.62	97.2% – 102.6%
	20	19.62 ± 0.21	1.09	
	50	51.04 ± 0.52	1.03	
Between-run ($n = 3$)				
Chlorogenic acid	40	39.66 ± 0.62	1.77	97.0% – 105.2%
	80	81.38 ± 1.27	1.64	
	150	156.20 ± 1.21	0.14	
Rutin	10	9.88 ± 0.08	0.62	97.2% – 103.9%
	20	19.84 ± 0.26	1.09	
	50	51.14 ± 0.15	1.03	

report of *E. elatior* inhibiting both enzymes [27] may be due to differences in extraction methods and assay conditions. Nor et al (2020) used a water extract prepared by an ultrasonic-assisted technique and a substrate concentration half that used in our study. These methodological differences are likely responsible for the variation observed in α-amylase activity.

Interestingly, EF-70 exhibited stronger α-glucosidase inhibition than ED-50 and ED-70, despite having lower chlorogenic acid and rutin contents. As a Zingiberaceae plant, *E. elatior* contains volatile compounds, including α-glucosidase-inhibiting monoterpenes such as pinene and limonene, which may degrade during heat drying, thereby reducing activity [28]. These findings suggest that other phytochemicals, such as volatile monoterpenes [29, 30] and phenolic compounds [31, 32], might contribute to EF-70's activity. Chlorogenic acid showed weaker α-glucosidase inhibition than acarbose, whereas rutin exhibited stronger inhibition, consistent with previous studies in *Morus alba* leaves [12] and *Syzygium samarangense* fruit [33], in which they were also identified as glucose-lowering agents.

Table 4 Content of chlorogenic acid and rutin in *E. elatior* extracts.

Extract	Content (mg/g; mean ± SD)	
	Chlorogenic acid	Rutin
EF-W	1.82 ± 0.24^{a}	0.96 ± 0.07^{j}
EF-50	$3.09 \pm 0.13^{b,c}$	$2.16 \pm 0.18^{g,h,i}$
EF-70	3.10 ± 0.39^{b}	2.57 ± 0.31^{h}
EF-95	0.99 ± 0.07^{a}	1.71 ± 0.04^{g}
ED-W	$5.63 \pm 0.21^{b,c}$	$1.82 \pm 0.05^{g,i}$
ED-50	9.46 ± 0.55^{f}	3.09 ± 0.11^{h}
ED-70	7.56 ± 0.21^{c}	3.10 ± 0.16^{h}
ED-95	2.40 ± 0.05^{d}	1.09 ± 0.00^{j}

Different alphabets above the values showed statistically significant differences (p-value < 0.05), calculated by Tukey's multiple comparison test. (chlorogenic acid: a–f; rutin: g–j)

In the *in silico* study, rutin showed the highest binding affinity with the greatest number of interactions, while chlorogenic acid exhibited binding energy comparable to that of acarbose. The number of interactions is directly related to the binding energy between protein and ligand [34]. Intermolecular interactions between the protein and ligand are crucial for stabilizing the energy of the docked ligand at the protein's active site, thereby contributing to the binding affinity of the complex [35]. Hydrogen and hydrophobic bonds help stabilize the protein-ligand complex at the target site [36]. On the other hand, unfavorable protein-ligand interactions (such as donor-donor or acceptor-acceptor interactions) reduce the complex's stability due to the repulsion between interacting molecules or atoms [37].

Regarding α-glucosidase (3A4A), previous studies have shown that acarbose interacted to the Asp215, Glu277, and Asp352 residues, which were characterized as catalytic residues in the α-glucosidase active site [38]. In this study, all compounds interacted with the catalytic residues, indicating their role in the inhibitory effects of α-glucosidase (3A4A): acarbose with Asp215, Glu277 and Asp352; chlorogenic acid with Asp242 and Glu277; and rutin with Asp242. The molecular docking study of *Saccharomyces* α-glucosidase (3A4A) correlated with the *in vitro* experiment, showing the binding affinity in the order of rutin > acarbose > chlorogenic acid. In human α-glucosidase (3L4Y), previous research identified Asp203, Asp327, Asp443, Arg526, Asp542, and His600 as the active site residues [39]. In this study, acarbose interacted with Asp203 and Asp542; chlorogenic acid with Asp203, Asp327 and Asp542, and Asp443; and rutin with Asp203. All the compounds demonstrated their inhibitory effects through molecular interactions with the catalytic residues at the enzyme's active site.

In previous studies on porcine α-amylase (1OSE), the key catalytic residues have been identified as Asp197, Glu233, and Asp300 [40]. In this study, acarbose interacted with Asp197 and Glu233; chlorogenic acid with Glu233; and rutin with Glu233 and Asp300. These findings suggest that all compounds influenced the enzyme-substrate interaction of α-amylase. However, *in vitro* results differed from *in silico* molecular docking study. Although rutin and chlorogenic acid showed *in silico* binding affinity to α-amylase comparable to that of acarbose, they exhibited ineffective activity against α-amylase *in vitro*. These differences highlighted the limitations of *in silico* study. Molecular docking is conducted based on computational simulations of protein and ligand structures, which exclude actual environmental factors such as the presence of water molecules and the dynamic nature of proteins and ligands. Therefore, the results from molecular docking have been reported to have a high false positive rate [41]. To achieve more accurate results, methodologies such as molecular dynamic simulations are recommended, as they can provide deeper insights into the interactions and stability of ligand-receptor complexes [42].

Comparative molecular docking demonstrated chlorogenic acid and rutin as potential human α-glucosidase inhibitors. Since these compounds showed low *in vitro* inhibitory activity against α-amylase, our focus shifted to the α-glucosidase. Both compounds showed lower binding affinity to human α-glucosidase (3L4Y) than to the experimental enzyme (3A4A), indicating a possibly reduced potency in humans. Thus, other human α-glucosidase inhibitory assays, such as cell-based Caco-2 model, should be further investigated [43]. Notably, chlorogenic acid and rutin displayed slightly stronger binding affinity to human α-glucosidase than acarbose, demanding further investigation to confirm their potential as human α-glucosidase inhibitors.

For HPLC analysis, we validated our previous HPLC method for determining chlorogenic acid and rutin [16]. Previous studies on *E. elatior* have used various markers and instruments, including UHPLC [6], LC-MS [14], HPLC [15, 16], and GC-MS [44]. This study is the first to validate an HPLC method for the α-glucosidase inhibitory markers of *E. elatior* flowers, chlorogenic acid and rutin, showing reliable results for quality control. The method supports as quality control of *E. elatior* as a traditional medicine, functional food, or dietary supplement, aiding future studies, clinical trials, and product development.

CONCLUSION

This study demonstrated that various extraction methods influenced inhibitory activity of *E. elatior* extracts on the tested enzymes, with the 70% ethanolic extract of fresh crude flowers showing the strongest α-glucosidase inhibition, whereas none exhibited activity against α-amylase. Chlorogenic acid and rutin demonstrated inhibitory activity against α-glucosidase, with

rutin exhibiting greater inhibitory potency compared to acarbose. Both *in silico* and *in vitro* studies confirmed that chlorogenic acid and rutin play a key role as α-glucosidase inhibition. Validation of the HPLC method for determining chlorogenic acid and rutin in the extract showed satisfactory validation results. This method can be applied as a reliable quality control approach for *E. elatior* flower extracts for further development of products, including traditional medicines, dietary supplements, and functional foods.

Appendix A. Supplementary data

Supplementary data associated with this article can be found at https://dx.doi.org/10.2306/scienceasia1513-1874.2025.094.

Acknowledgements: This work was supported by the Department of Medical Sciences, Ministry of Public Health, Thailand, for providing necessary facilities and financial support to conduct this research. We are grateful to Yala Horticultural Research Center, Yala, Thailand, for providing the plant utilized in this study. We also appreciate the Clinical Research Center at Thammasat University for providing English manuscript editing services by an English professor.

REFERENCES

1. Genuth SM, Palmer JP, Nathan DM (2018) Classification and diagnosis of diabetes. In: Cowie CC, Casagrande SS, Menke A, Cissell MA, Eberhardt MS, Meigs JB, Gregg EW, Knowler WC, et al (eds) *Diabetes in America*, 3rd edn, National Institute of Diabetes and Digestive and Kidney Diseases, USA, pp 2–6.
2. Leslie RD, Palmer J, Schloot NC, Lernmark A (2016) Diabetes at the crossroads: relevance of disease classification to pathophysiology and treatment. *Diabetologia* **59**, 13–20.
3. Rosak C, Mertes G (2012) Critical evaluation of the role of acarbose in the treatment of diabetes: patient considerations. *Diabetes Metab Syndr Obes* **5**, 357–367.
4. Chiasson JL, Josse RG, Gomis R, Hanefeld M, Karasik A, Laakso M (2003) Acarbose treatment and the risk of cardiovascular disease and hypertension in patients with impaired glucose tolerance: the STOP-NIDDM trial. *JAMA* **290**, 486–494.
5. Ibrahim H, Setyowati FM (1999) *Etlingera*. In: de Guzman CC, Siemonsma JS (eds) *Plant Resources of South-East Asia*, Backhuys Publishers, The Netherlands, pp 123–126.
6. Ghasemzadeh A, Jaafar HZE, Rahmat A, Ashkani S (2015) Secondary metabolites constituents and antioxidant, anticancer and antibacterial activities of *Etlingera elatior* (Jack) R.M.Sm grown in different locations of Malaysia. *BMC Complement Altern Med* **15**, 335.
7. Juwita T, Pakpahan WHP, Puspitasari IM, Mekar Saptarini NM, Levita J (2020) Anti-inflammatory activity of *Etlingera elatior* (Jack) R.M. Smith flower on gastric ulceration-induced Wistar rats. *Pak J Biol Sci* **23**, 1193–1200.
8. Whangsomnuek N, Mungmai L, Mengamphan K, Amornlerdpison D (2019) Efficiency of skin whitening cream containing *Etlingera elatior* flower and leaf extracts in volunteers. *Cosmetics* **6**, 39.
9. Lachumy SJT, Sasidharan S, Sumathy V, Zuraini Z (2010) Pharmacological activity, phytochemical analysis and toxicity of methanol extract of *Etlingera elatior* (torch ginger) flowers. *Asia Pac J Trop Med* **3**, 769–774.
10. Nor NAM, Azmi NA, Noordin L, Bakar NHA, Ahmad WANW (2019) Aqueous extract of *Etlingera elatior* flowers improved blood glucose control, kidney function and histology of streptozotocin-induced diabetic rat. *J Sustain Sci Manag* **14**, 80–91.
11. Chen SC, Yang CS, Chen JJ (2022) Main bioactive components and their biological activities from natural and processed rhizomes of *Polygonum sibiricum*. *Antioxidants (Basel)* **11**, 1383.
12. Hunyadi A, Martins A, Hsieh TJ, Seres A, Zupkó I (2012) Chlorogenic acid and rutin play a major role in the *in vivo* anti-diabetic activity of *Morus alba* leaf extract on type II diabetic rats. *PLoS One* **7**, e50619.
13. Chan EW, Lim YY, Tan SP (2011) Standardized herbal extract of chlorogenic acid from leaves of *Etlingera elatior* (Zingiberaceae). *Pharmacognosy Res* **3**, 178–184.
14. Ge L, Yong JWH, Tan SN, Li SP (2020) Simultaneous extraction, separation, isolation and identification of endogenous components from *Etlingera elatior* by pressurized matrix solid-phase dispersion using liquid chromatography-mass spectrometry. *J Chromatogr A* **1611**, 460604.
15. Firdhauzi A, Yupanqui CT, Setyaningsih W, Seechamnanturakit V (2024) Optimization of ultrasound-assisted extraction using Box–Behnken design, method validation, and analysis of phytochemicals from drying treatments in the application of *Etlingera elatior* inflorescence. *Funct Food Health Dis* **14**, 311–333.
16. Sinsuebpol C, Nakpheng T, Srichana T, Sawatdee S, Pipatrattanaseree W, Burapapadh K, Changsan N (2023) Assessing the anti-aging and wound healing capabilities of *Etlingera elatior* inflorescence extract: A comparison of three inflorescence color varieties. *Molecules* **28**, 7370.
17. Gowri PM, Tiwari AK, Ali AZ, Rao JM (2007) Inhibition of alpha-glucosidase and amylase by bartogenic acid isolated from *Barringtonia racemosa* Roxb. seeds. *Phytother Res* **21**, 796–799.
18. Ademiluyi AO, Oboh G (2013) Soybean phenolic-rich extracts inhibit key enzymes linked to type 2 diabetes (α-amylase and α-glucosidase) and hypertension (angiotensin I converting enzyme) *in vitro*. *Exp Toxicol Pathol* **65**, 305–309.
19. Berman HM, Westbrook J, Feng Z, Gilliland G, Bhat TN, Weissig H, Shindyalov IN, Bourne PE (2000) The protein data bank. *Nucleic Acids Res* **28**, 235–242.
20. Kulkarni AA, Kamble RP (2022) α-amylase inhibitory secondary metabolites from *Artemisia pallens* Wall ex DC: biochemical and docking studies. *Biol Life Sci Forum* **11**, 73.
21. Ahmed S, Ali MC, Ruma RA, Mahmud S, Paul GK, Saleh MA, Alshahrani MM, Obaidullah AJ, et al (2022) Molecular docking and dynamics simulation of natural compounds from betel leaves (*Piper betle* L.) for investigating the potential inhibition of alpha-amylase and alpha-glucosidase of type 2 diabetes. *Molecules* **27**, 4526.
22. Peytam F, Takalloobanafshi G, Saadattalab T, Norouzbahari M, Emamgholipour Z, Moghimi S, Firoozpour L, Bijanzadeh HR, et al (2021) Design, synthesis, molecular docking, and *in vitro* α-glucosidase inhibitory activi-

ties of novel 3-amino-2,4-diarylbenzo[4,5]imidazo[1,2-*a*]pyrimidines against yeast and rat α-glucosidase. *Sci Rep* **11**, 11911.

23. Sim L, Jayakanthan K, Mohan S, Nasi R, Johnston BD, Pinto BM, Rose DR (2010) New glucosidase inhibitors from an ayurvedic herbal treatment for type 2 diabetes: structures and inhibition of human intestinal maltase-glucoamylase with compounds from *Salacia reticulata*. *Biochemistry* **49**, 443–451.
24. Kim S, Chen J, Cheng T, Gindulyte A, He J, He S, Li Q, Shoemaker BA,et al (2021) PubChem in 2021: new data content and improved web interfaces. *Nucleic Acids Res* **49**, D1388–D1395.
25. Dallakyan S, Olson AJ (2015) Small-molecule library screening by docking with PyRx. *Methods Mol Biol* **1263**, 243–250.
26. ICH (2005) *Validation of Analytical Procedures: Text and Methodology Q2(R1)*. The International Council for Harmonisation, Switzerland.
27. Nor NAM, Noordin L, Bakar NHA, Ahmad WANW (2020) Evaluation of antidiabetic activities of *Etlingera elatior* flower aqueous extract *in vitro* and *in vivo*. *J Appl Pharm Sci* **10**, 43–51.
28. Maurya AK, Vashisath S, Aggarwal G, Yadav V, Agnihotri VK (2022) Chemical diversity and α-glucosidase inhibitory activity in needles essential oils of four *Pinus* species from northwestern Himalaya, India. *Chem Biodivers* **19**, e202200428.
29. Thouri A, Chahdoura H, El Arem A, Omri Hichri A, Ben Hassin R, Achour L (2017) Effect of solvents extraction on phytochemical components and biological activities of Tunisian date seeds (var. Korkobbi and Arechti). *BMC Complement Altern Med* **17**, 248.
30. Charaslertrangsi T, Yanukun K, Suksamrarn A, Piyachaturawat P, Sutjarit N (2025) Suppression of TNF-α-induced dysregulation of adipocytokine and insulin signaling in 3T3-L1 adipocytes by a diarylheptanoid from *Curcuma comosa*. *ScienceAsia* **51**, ID 2025040.
31. Seubsasana S, Dechayont B, Pipatrattanaseree W, Malisorn N (2023) Antioxidant activity, α-glucosidase inhibition, and phytochemical profiling of *Belosynapsis ciliata* (Blume) R.S.Rao extracts. *ScienceAsia* **49**, 15–21.
32. Boonmee A, Moonrungsee N, Kasemsuk T, Puckdee W, Komonpanich P, Kunsook C, Khamchatra N, Nakeim S, et al (2023) The antioxidant activities and inhibitory effects on α-glucosidase and α-amylase of ethanolic and aqueous extracts from various parts of Thai *Caesalpinia sappan* L. *ScienceAsia* **49**, 618–626.
33. Suksri K, Yingngam B, Muangchan N (2023) Optimization of phenolic extraction from *Syzygium samarangense* fruit and its protective properties against glucotoxicity-induced pancreatic β-cell death. *ScienceAsia* **49**, 529–540.
34. Lu Y, Wang Y, Xu Z, Yan X, Luo X, Jiang H, Zhu W (2009) C–X$\cdots$H contacts in biomolecular systems: how they contribute to protein–ligand binding affinity. *J Phys Chem B* **113**, 12615–12621.
35. Patil R, Das S, Stanley A, Yadav L, Sudhakar A, Varma AK (2010) Optimized hydrophobic interactions and hydrogen bonding at the target–ligand interface leads the pathways of drug-designing. *PLoS One* **5**, e12029.
36. Davis AM, Teague SJ (1999) Hydrogen bonding, hydrophobic interactions, and failure of the rigid receptor hypothesis. *Angew Chem Int Ed Engl* **38**, 736–749.
37. Dhorajiwala T, Halder S, Samant L (2019) Comparative *in silico* molecular docking analysis of L-threonine-3-dehydrogenase, a protein target against African trypanosomiasis using selected phytochemicals. *J Appl Biotechnol Rep* **6**, 101–108.
38. Tang H, Ma F, Zhao D (2019) Exploring the effect of salvianolic acid C on α-glucosidase: inhibition kinetics, interaction mechanism and molecular modelling methods. *Process Biochem* **78**, 178–188.
39. Ibrahim MA, Bester MJ, Neitz AW, Gaspar ARM (2018) Rational *in silico* design of novel α-glucosidase inhibitory peptides and *in vitro* evaluation of promising candidates. *Biomed Pharmacother* **107**, 234–242.
40. Ogunyemi OM, Gyebi GA, Saheed A, Paul J, Nwaneri-Chidozie V, Olorundare O, Adebayo J, Koketsu M, et al (2022) Inhibition mechanism of alpha-amylase, a diabetes target, by a steroidal pregnane and pregnane glycosides derived from *Gongronema latifolium* Benth. *Front Mol Biosci* **9**, 866719.
41. Khanjiwala Z, Khale A, Prabhu A (2019) Docking structurally similar analogues: dealing with the false-positive. *J Mol Graph Model* **93**, 107451.
42. Karplus M, McCammon JA (2002) Molecular dynamics simulations of biomolecules. *Nat Struct Biol* **9**, 646–652.
43. Huang YN, Zhao YL, Gao XL, Zhao ZF, Jing Z, Zeng WC, Yang R, Peng R, et al (2010) Intestinal α-glucosidase inhibitory activity and toxicological evaluation of *Nymphaea stellata* flowers extract. *J Ethnopharmacol* **131**, 306–312.
44. Anzian AB, Rashidah S, Nazamid S, Sapawi CWN, Hussin ASM (2017) Chemical composition and antioxidant activity of torch ginger (*Etlingera elatior*) flower extract. *Food Appl Biosci J* **5**, 32–49.

Appendix A. Supplementary data

Table S1 Grid parameters in molecular docking between enzymes and ligands.

Protein	Grid center	Grid space (Å)
1OSE	X = 35.66, Y = 37.37, Z = −1.20	25
3BAJ	X = 10.15, Y = 15.83, Z = 41.12	25
3A4A	X = 21.52, Y = −7.70, Z = 23.56	25
3L4Y	X = −2.01, Y = −19.26, Z = −20.85	25

Table S2 Docking scores and molecular interactions of acarbose and the markers of *E. elatior* extract, chlorogenic acid and rutin.

Enzyme (PDB ID)	Ligand	Binding energy (kcal/mol)	Interaction residue of target					
			No.	Hydrogen bond interaction	No.	Hydrophobic interaction	No.	Unfavorable interaction
Porcine amylase (1OSE)	Acarbose	−8.0	6	Gln63, Gly104, Val163, Asp197, Asp300, His305	1	Trp59	1	Glu233
	Chlorogenic acid	−8.1	1	Glu233	2	Trp59, Val163	1	Gln63
	Rutin	−9.4	2	Glu233, His299, Asp300	7	Trp59(2), Val163, Asp300, His305(2), Asp356	1	Gln63
Human amylase (3BAJ)	Acarbose	−7.7	7	Gln63(2), Tyr151, Thr163(2), Glu233, Asp300	1	His201	0	–
	Chlorogenic acid	−8.0	7	Gln63(2), Thr163, Asp197, Glu233, His299, Asp300	3	Trp59, Tyr62 Asp197	1	Arg195
	Rutin	−9.4	5	Thr163, Lys200, Glu233, His299, His305	8	Tyr62(2), Trp59, Tyr151, Leu162, Lys200, ILE235, Asp300	0	–
S. cerevisiae glucosidase (3A4A)	Acarbose	−9.0	9	Asp69, Tyr158, Arg213, Asp215, Ser240, Asp242, Glu277, His280, Glu411	8	Tyr158, Phe178, Glu277, His280, ASP215, Asp352(2), Glu411	2	Gln279, Arg442
	Chlorogenic acid	−8.8	7	Lys156, Ser240, Asp242, Glu277, Asp352, Gln353, Arg442	2	Tyr158, Arg315	0	–
	Rutin	−10.4	6	Ser240 (2), Asp242, His280, Leu313(2)	5	Asp242, Arg315(2), Glu411, Arg442	1	Pro312
Human glucosidase (3L4Y)	Acarbose	−6.3	6	Asp203(2), Phe450(2), Asp542, Tyr605	1	Asp203	0	–
	Chlorogenic acid	−7.3	4	Asp203, Thr205, Asp327, Asp542	1	Asp443	0	–
	Rutin	−8.9	6	Arg202, Asp203(2), Thr205(2), Met444	4	Trp406, Phe450(2), Ala576	0	–

Table S3 Limit of detection (LOD) and limit of quantitation (LOQ) of chlorogenic acid and rutin.

Compound	Linear range (µg/ml)	Limit of detection (µg/ml)	Limit of quantitation (µg/ml)
Chlorogenic acid	20 – 250	0.2	1.0
Rutin	10 – 100	0.125	0.5

Table S4 Intermediate precision evaluated between days, columns, and instruments.

Compound	Spiked concentration	Intermediate precision (RPD, %)		
	(µg/ml)	Day*	Column	Instrument
Chlorogenic acid	40	0.77	3.24	0.72
	80	1.59	0.28	3.36
	150	0.14	3.51	0.76
Rutin	10	1.18	1.64	2.46
	20	1.50	5.62	3.76
	50	0.72	0.48	2.43

* The results showed %RSD for three different days.

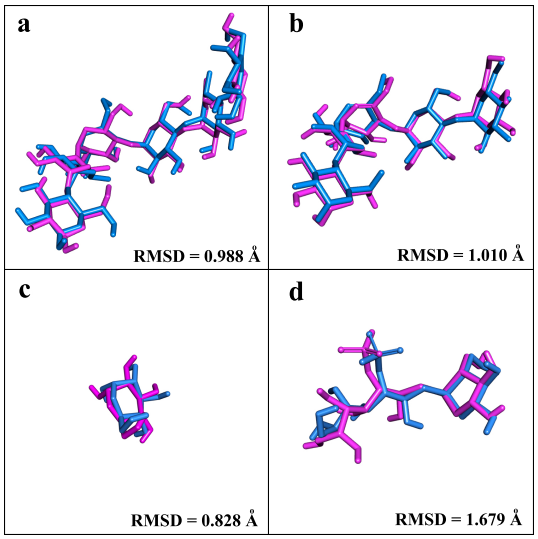

Fig. S1 Superimposition of the 3D structures of the re-docked ligand (purple) with the native ligand (blue) for (a) porcine α-amylase (1OSE), (b) human pancreatic α-amylase (3BAJ), (c) *S. cerevisiae* α-glucosidase (3A4A), and (d) human α-glucosidase (3L4Y).

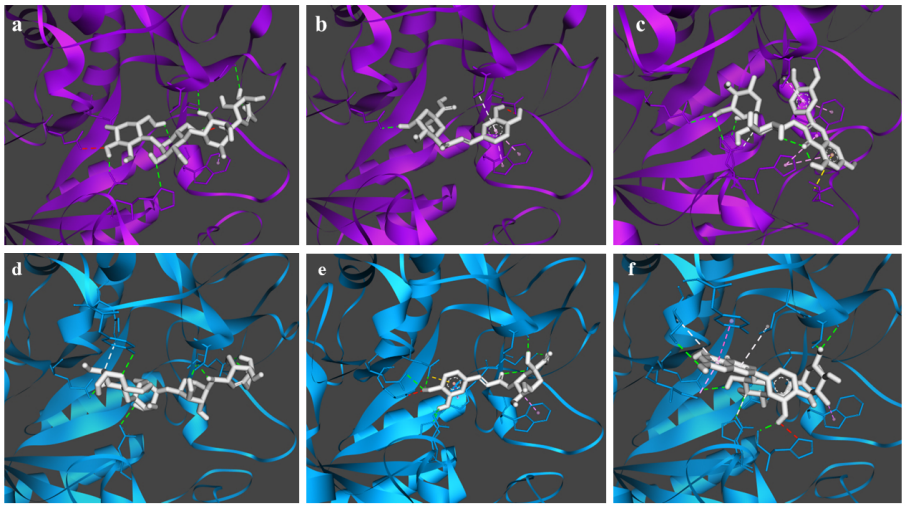

Fig. S2 3D models of α-amylase with docked ligands at the active sites. Proteins: (a–c) porcine pancreatic α-amylase (1OSE) and (d–f) human pancreatic α-amylase (3BAJ). Ligands: acarbose (a, d); chlorogenic acid (b, e); rutin (c, f).

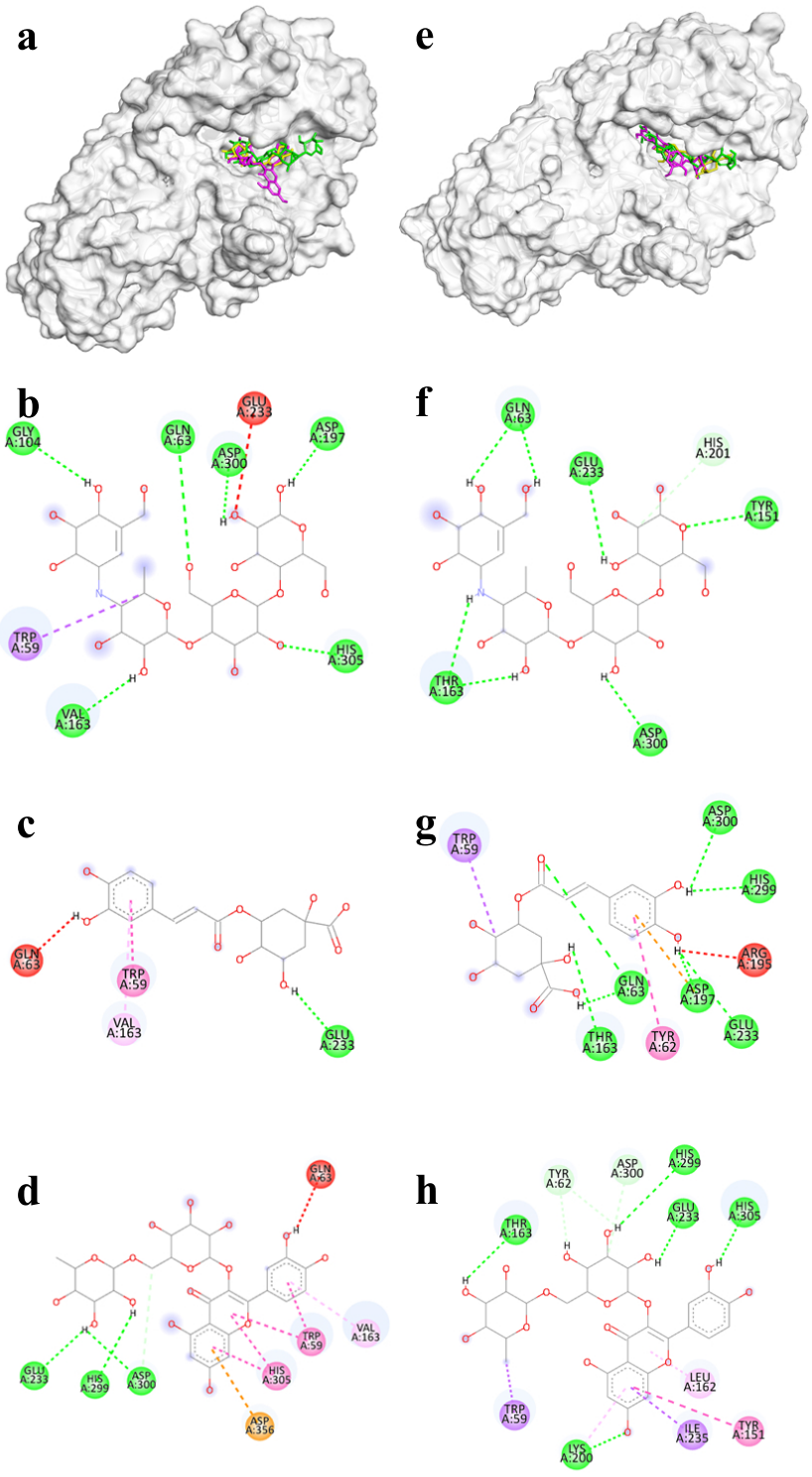

Fig. S3 3D models of α-amylase with docked ligands (acarbose, chlorogenic acid, and rutin) at the active sites: (a) porcine pancreatic α-amylase (1OSE) and (e) human pancreatic α-amylase (3BAJ). 2D predicted binding interactions of chlorogenic acid, rutin, and acarbose at the active sites of 1OSE (b, c, and d, respectively) and 3BAJ (f, g, and h, respectively). Types of ligand-protein interaction are classified by color: green = hydrogen bonding; pink = Pi-Pi stacked; pale pink = Pi-alkyl; purple = Pi-Sigma; brown = Pi-Anion; red = unfavorable acceptor-acceptor or donor-donor.

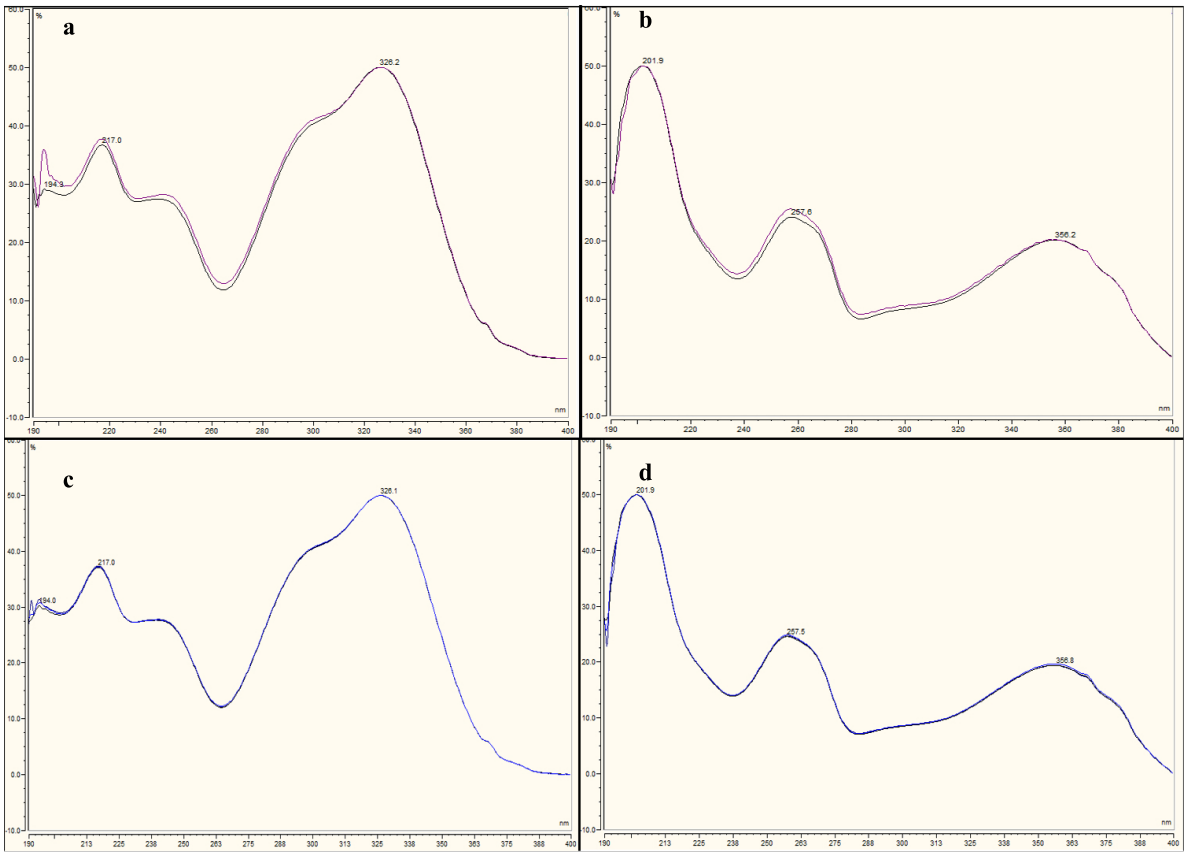

Fig. S4 Comparative UV spectra of the responsive peaks in the standard solution and sample solution (a, b) and of the peak in sample solution at peak-start, peak-apex, and peak-end (c, d).

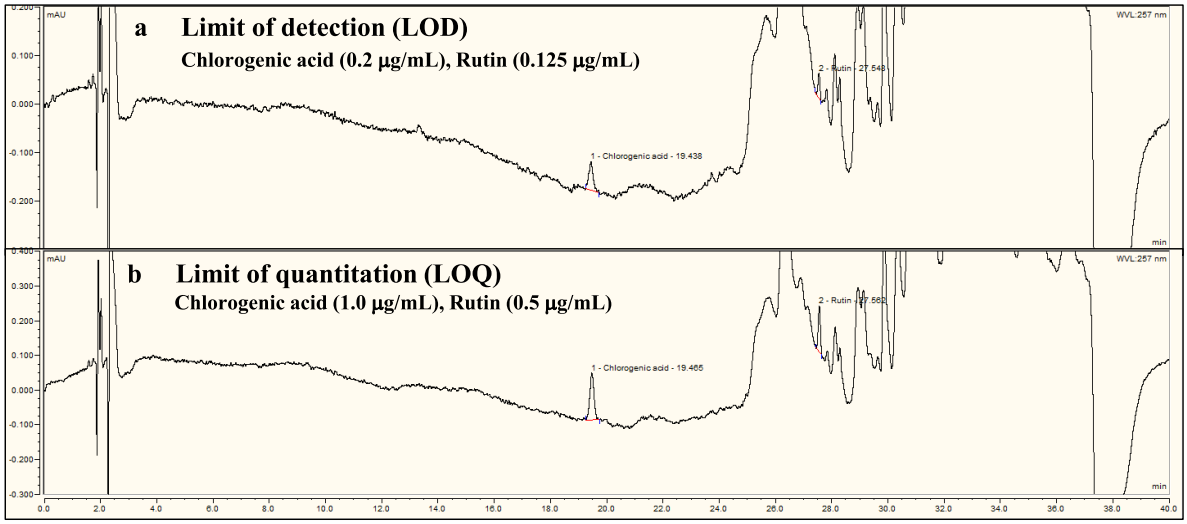

Fig. S5 HPLC chromatograms of the standard solution at the limit of detection (a) and the limit of quantitation (b).